RSC Advances

ROYAL SOCIETY OF CHEMISTRY

www.rsc.org/advances

Green synthesis of fluorescent nitrogen/sulfur-doped carbon dots and investigation of their properties by HPLC coupled with mass spectrometry†

Qin Hu,[a] Man Chin Paau,[a] Yan Zhang,[b] Xiaojuan Gong,[b,‡] Lei Zhang,[b,‡] Dongtao Lu,[b,‡] Yang Liu,[b,‡]
5 Qiaoling Liu,[b,‡] Jun Yao*[c] and Martin M.F. Choi*[a]

A fast and green approach to synthesise ultrasmall nitrogen (*N*) and sulfur (*S*)-doped carbon dots (*N*,*S*-C-dots) by microwave-assisted pyrolysis of precursors of rice as carbon source and *N*-acetyl-L-cysteine
10 (NAC) as *N* and *S* dopants has been developed. The obtained *N*,*S*-C-dots were fully characterised by elemental analysis, Fourier transform infrared spectroscopy, x-ray photoelectron spectroscopy, transmission electron microscopy, UV-vis absorption and photoluminescence (PL) spectroscopy. The undoped C-dots (derived from rice only) and *N*,*S*-C-dots possess different chemical compositions, sizes and spectral properties. With the assistance of high-performance liquid chromatography coupled with
15 fluorescence detection (HPLC-FD), the effect of different mass ratios of NAC to rice (NAC/rice) on *N*,*S*-C-dots was investigated. Higher NAC/rice benefits the generation of *N*,*S*-C-dots with stronger fluorescence emission. In addition, the HPLC separated *N*,*S*-C-dots fractions were collected and further characterised by mass spectrometry, UV-vis absorption and PL spectroscopy, showing that the structural changes induced by doping with heteroatoms *N* and *S* plays a key role in regulating the PL properties of
20 the *N*,*S*-C-dots. This work highlights the merits of synthesising *N*,*S*-C-dots from readily available natural bioresource and applying modern HPLC-FD technology to study the effect of doped heteroatoms on *N*,*S*-C-dots properties.

Introduction

The recently discovered carbon dots (C-dots) constitute a
25 fascinating class of nanoscale particles with typical diameters less than 10 nm.[1-3] Up to now C-dots have drawn considerable interests owing to their outstanding optical properties, robust chemical inertness, low cytotoxicity and excellent biocompatibility as compared to other semiconductor quantum
30 dots (QDs) with heavy metals and chalcogens.[4,5] Strikingly the C-dots reported so far are hydrophilic in nature and appear to be a promising alternative to semiconductor QDs in the fields of optoelectronic devices, biological labelling, drug delivery, sensors and biomedicine.[6-8]
35 Impressive progresses have been made on the synthesis of C-dots with methods such as electrochemical oxidation,[9,10] laser ablation,[5,11,12] hydrothermal synthesis,[13-15] pyrolysis,[2,3,16] and microwave-assisted heating.[17-20] Nevertheless, most of these synthetic methods suffer from shortcomings such as expensive
40 equipment required, time-consuming procedures, slow and high cost. Recently Li *et al.*[21] synthesised C-dots by simply mixing monosaccharide with basic solutions without additional energy input or external heating. More importantly, the synthesis of C-dots with naturally available bioresources is attractive in the area
45 of nanotechnology. For example, carbonization of orange juice,[13] potato,[22] protein,[23] willow bark,[24] *trapa bispinosa* peel,[25] hair fibre,[26] and *bombyx mori* silk[27] offer facile routes for synthesis of fluorescent C-dots. To date, there is a great interest in incorporating heteroatoms into C-dots framework to enhance the

50 photoluminescence (PL) properties of C-dots. So far numerous strategies have been conducted to produce C-dots containing nitrogen. However, reports about fabricating C-dots containing other heteroatoms whether singly or dually doped with other dopants are still limited. Xu *et al.*[28] synthesised phosphate
55 functionalized two colour C-dots through acidic oxidation of sucrose by H_3PO_4. Wang *et al.*[29] fabricated phosphorus-containing C-dots with strong green fluorescence from phytic acid and ethylenediamine. Sun *et al.*[26] produced luminescent sulfur and nitrogen-co-doped C-dots from hair fibre. Dong *et al.*[30]
60 reported the preparation of highly fluorescent C-dots doped with nitrogen and sulfur atoms (*N*,*S*-C-dots) from citric acid and L-cysteine. Nevertheless, exploring new synthetic routes for synthesis of C-dots doped with heteroatoms is still a tricky challenge.
65 In the present work, we report a "green" and facile approach to synthesise strongly fluorescent *N*,*S*-C-dots by microwave-assisted pyrolysis of rice and *N*-acetyl-L-cysteine (NAC) as precursors. Rice rich in carbon atoms can serve as an excellent carbon source. NAC comprising both N and S atoms can function as dopants for
70 C-dots. It possesses good water-solubility, and is non-toxic and cost-effective. The synthesis is completed in a domestic microwave oven within 30 min. Doping N and S into C-dots greatly increases the quantum yield (Φ_S) of C-dots. The obtained *N*,*S*-C-dots solution exhibits homogeneous phase without any
75 noticeable precipitation at ambient conditions for six months, indicating their long-term colloidal stability. Herein, high-

performance liquid chromatography coupled with fluorescence detection (HPLC-FD) has been successfully applied to study the effect of mass ratio of NAC to rice (NAC/rice) on the as-synthesised *N,S*-C-dots products. Remarkably, HPLC-FD is able to identify how different NAC/rice affects the PL of the *N,S*-C-dots products. Finally, the HPLC separated fractions of the undoped C-dots (derived from rice only) and *N,S*-C-dots were collected and characterised by matrix-assisted laser desorption/ionisation time-of-flight mass spectrometry (MALDI-TOF MS), UV-vis absorption and PL spectroscopy, probing the structural changes and PL of *N,S*-C-dots induced by doping with N and S. To our knowledge, this is the first report on microwave-assisted synthesis of *N,S*-C-dots using rice and NAC as precursors and application of HPLC-FD technique to analyse separated *N,S*-C-dots fractions. Our work certainly adds to the database on the synthesis of C-dots from natural resource and provokes better understanding of the as-synthesised C-dots product.

Materials and methods

Materials
Rice was purchased from the local market in Hong Kong. Ammonium acetate (99.99 %) and *N*-acetyl-L-cysteine (99%) were from International Laboratory (San Bruno, CA, USA). HPLC-grade methanol (MeOH) and AR-grade acetone were from Labscan (Bangkok, Thailand). 2,5-Dihydroxbenzoic acid (DHB) was purchased from Sigma (St. Louis, MO, USA). Distilled deionised (DDI) water was obtained from a Millipore Milli-Q-RO4 water purification system with a resistivity higher than 18 $M\Omega \cdot cm$ (Bedford, MA, USA). All reagents of analytical reagent grade or above were used as received without further purification.

Synthesis of C-dots sample
N,S-C-dots were synthesised by microwave-heating rice and NAC together. Before synthesis, rice was put in a Waring Laboratory Micronizer FPC70 (Waring Products Division, New Hartford, Conn, USA) to obtain fine rice powder with diameter less than 1.0 mm. In a typical synthetic procedure, 0.50 g rice powder, various amounts of NAC (0.00–0.40 g) and 2.0 mL DDI water were loaded into a 10-mL beaker. The reagents were thoroughly mixed and heated in a domestic microwave oven (800 W) for 30 min. After carbonisation, the beaker was cooled to room temperature. The resulting dark brown solid product was extracted with 3.0 mL DDI water and sonicated for 1 min to obtain the water-soluble *N,S*-C-dots. Then 50.0 mL acetone was added to the solution and it was centrifuged at 6000 rpm for 20 min to remove any unreacted raw materials. The acetone/water in the solution was removed by a stream of nitrogen (N_2) to obtain the solid brown residues. The *N,S*-C-dots crude product was re-dissolved in water and purified by a Spectrum Laboratories (Rancho Dominguez, CA, USA) dialysis membrane tube (molecular weight cut-off 500–1000 Da) in DDI water with stirring and recharging with fresh DDI water every 24 h for 3 days. Finally, the clear aqueous yellow solution was lyophilized to obtain the dry *N,S*-C-dots product. Undoped C-dots synthesised with rice only were also prepared for comparison. The undoped C-dots solution appears reddish brown while the *N,S*-C-dots solution is light yellow. Apparently, there are differences between the undoped C-dots and *N,S*-C-dots.

Apparatus
The elemental analysis was carried out on an Elementar Analysensysteme vario EL cube organic elemental analyser (Hanau, Germany). The FTIR spectra were performed on a Perkin-Elmer Paragon 1000 FTIR spectrometer (Waltham, MA, USA). The X-ray photoelectron spectra (XPS) were acquired on a Leybold Heraeus SKL-12 X-ray photoelectron spectrometer (Shenyang, China). Spectra were processed by the Casa XPS v.2.3.12 software using a peak-fitting routine with symmetrical Gaussian-Lorentzian functions. The transmission electron microscopic (TEM) images were acquired on a JEOL JEM-2010 transmission electron microscope (Tokyo, Japan) with an accelerating voltage of 300 kV. The UV-vis absorption spectra were recorded on a Varian Cary 300 Scan UV-vis absorption spectrophotometer (Palo Alto, CA, USA) and the PL spectra were acquired on a Photon Technology International QM4 spectrofluorometer (Birmingham, NJ, USA).

High-performance liquid chromatographic separation
Chromatographic separation was conducted on a Waters (Milford, MA, USA) instrument comprising a 2695 separation module coupled with a 2996 photodiode array detector (PDA) and a 2475 multi-wavelength fluorescence detector. The fluorescence chromatograms were acquired by monitoring the fluorescence detector at excitation/emission wavelengths of 340/400 nm. The PDA was used to *in-situ* capture the UV-vis absorption spectra of the HPLC separated *N,S*-C-dots fractions. An Agilent XDB-C18 HPLC column (150 x 4.6 mm i.d. stainless steel) packed with 5-μm octadecyl (C18) bonded silica with 80-Å pore size (Santa Clara, CA, USA) was used for chromatographic separation. The *N,S*-C-dots samples (1.0 mg/mL) were filtered through Alltech 0.45 μm, 13 mm i.d. cellulose acetate syringe filters (Deerfield, IL, USA) prior to injection. The mobile phases were prepared with binary mixtures of (A) MeOH and (B) 10 mM ammonium acetate buffer (pH 4.5). All HPLC analytical work was performed under isocratic elution with A and B (1:99 v/v) as the mobile phase. The flow rate was set at 0.80 mL/min, the injection volume was 20 μL and the column temperature was maintained at $25 \pm 1\ °C$.

Mass spectrometry
The MALDI-TOF MS of each *N,S*-C-dots HPLC fraction was conducted on a Bruker Autoflex MALDI-TOF mass spectrometer (Bremen, Germany). The collected HPLC fractions were dried by a stream of N_2 gas and re-dissolved in 5.0 μL DDI water. Then 4.0 μL of each HPLC fraction was mixed with a 4.0 μL 1.0 M DHB solution in MeOH/water (1:1 v/v). 2.0 μL of this solution was deposited on a MALDI target plate for two times separately. The sample was air-dried and was then inserted into the instrument. The MALDI-TOF MS were acquired in positive ionisation mode under a pulsed N_2 laser at 337 nm. In general, 500 laser shots were averaged for each spectrum.

Results and discussion

Characterisation of the as-synthesised *N,S*-C-dots
Four types of water-soluble *N,S*-C-dots were synthesised using various NAC/rice: 0.20, 0.40, 0.60, and 0.80. They all possess similar spectral characteristics but different emission intensities. Among them, the *N,S*-C-dots synthesised with NAC/rice of 0.80 produces the strongest fluorescence. As such, it was chosen for further characterisation and studies. Higher NAC/rice (> 0.80) does not improve the fluorescence of the *N,S*-C-dots and is not discussed in this work.

The doping of heteroatoms into *N,S*-C-dots was initially probed by elemental analysis in Table S1A (†ESI), revealing that the undoped C-dots are mainly composed of carbon (C), hydrogen (H) and oxygen (O) whereas the *N,S*-C-dots contain C, H, O, N, and S. The elemental content of the undoped C-dots differs

significantly from the *N*,*S*-C-dots. Higher N and S contents and less O content are found for the *N*,*S*-C-dots. For ease of comparison, the elemental contents of the C-dots are expressed in terms of relative number of atom as depicted in Table S1B†. The empirical formulae for the undoped C-dots and the *N*,*S*-C-dots are $C_{12}H_{22}O_{12}$ and $C_{13}H_{23}O_9N_2S$, respectively. The undoped C-dots and the *N*,*S*-C-dots contain almost the same number of C atoms. However, the numbers of O, N and S atoms in the *N*,*S*-C-dots differ significantly from that of the undoped C-dots. Three more O atoms are found in the undoped C-dots. By contrast, two N and one S atoms are found in the *N*,*S*-C-dots but not in the undoped C-dots. In other words, the three O atoms in the undoped C-dots were replaced by the N and S atoms in the *N*,*S*-C-dots after passivation with NAC, indicating that the N and S originated from NAC could co-dope into C-dots.
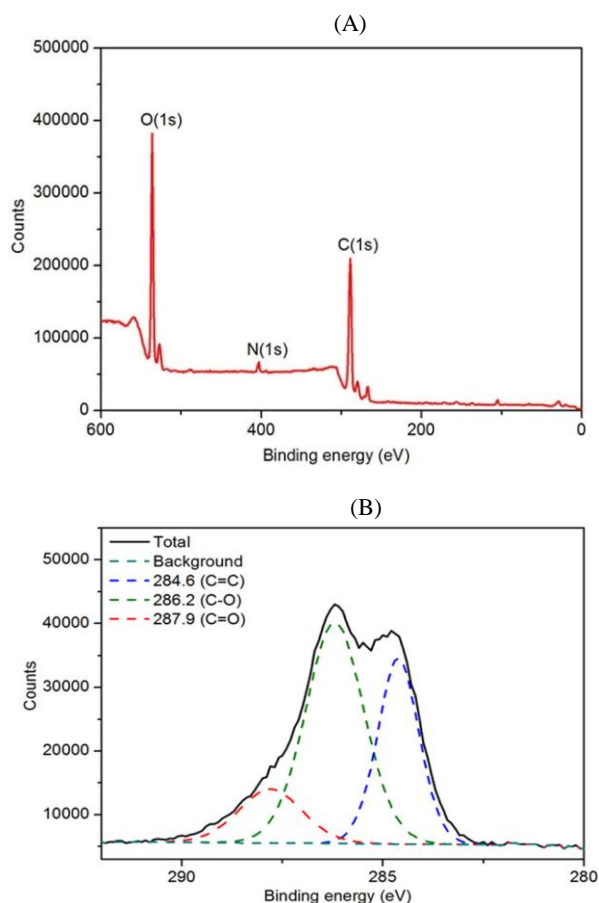

Fig. 1 (A) XPS survey scan and (B) C1s XPS spectrum of undoped C-dots.

IR measurement was used to confirm the doping of N and S into C-dots and investigate the differences in surface functionality of the two kinds of C-dots. Fig. S1† depicts the IR spectra of the undoped C-dots (spectrum *a*) and the *N*,*S*-C-dots (spectrum *b*). A broad absorption peak attributing to the O–H stretching (~3238–3470 cm^{-1}) and sharp absorption peaks corresponding to C–H (2930 cm^{-1}), C–O (1152 cm^{-1}), and C–O–C stretching (1021 cm^{-1}) are found for both undoped C-dots and *N*,*S*-C-dots. These functional groups are believed to be derived from rice as their carbon sources. The IR spectrum of rice possessing these functionalities is displayed in Fig. S2A†. More importantly, the characteristic absorption peaks C=O stretching (1716 cm^{-1}), amido CON–H bending (1545 cm^{-1}), amido CO–N (1375 cm^{-1}) and C–S (1081 cm^{-1}) stretching are identified in the *N*,*S*-C-dots,

suggesting the presence of carboxylic, amido and alkyl sulfide functionalities on the *N*,*S*-C-dots. The disappearance of the S–H stretching (2550 cm^{-1}) band in *N*,*S*-C-dots indicates that the initial S–H in NAC has been decomposed and S was incorporated into the *N*,*S*-C-dots.
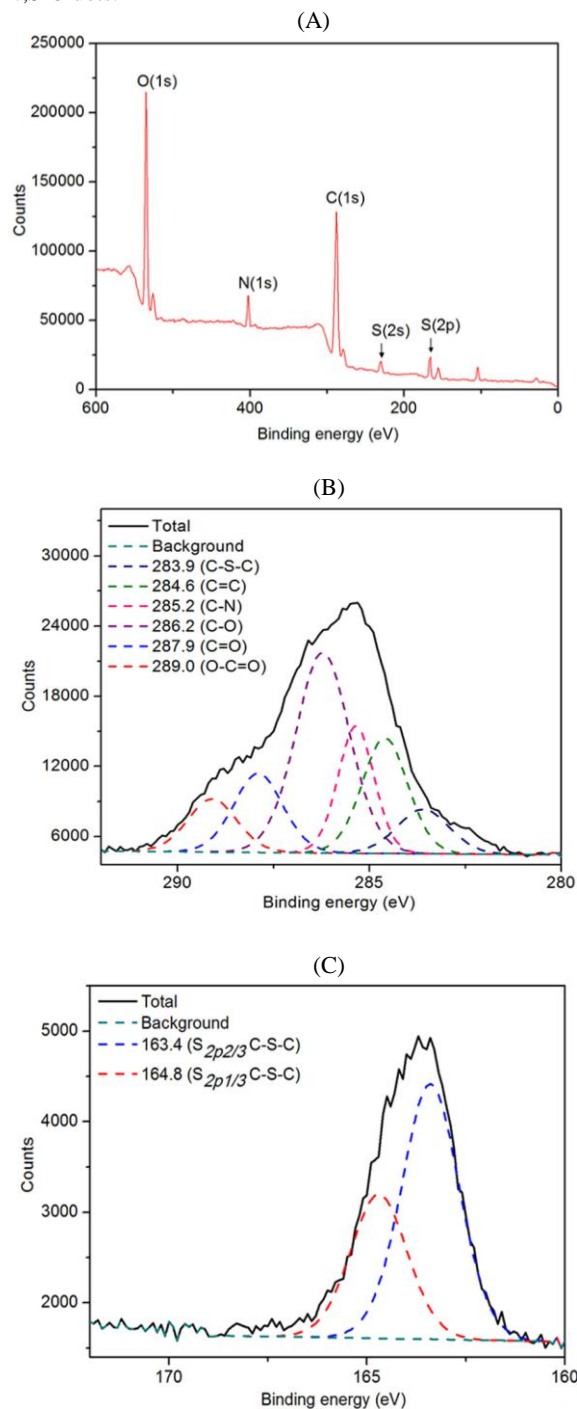

Fig. 2 (A) XPS survey scan, (B) C1s and (C) S2p XPS spectra of *N*,*S*-C-dots

The IR of NAC is shown in Fig. S2B† for comparison. Interestingly, an absorption peak associated with the C=O stretching (1716 cm^{-1}) which is absent from the IR spectrum of rice is observed in the undoped C-dots, suggesting the possible oxidation of carbon. In addition, the IR spectra of both undoped C-dots and *N*,*S*-C-dots possess a distinctive absorption peak at

1653 cm^{-1}, indicating the formation of C=C unsaturated bonds in the carbon cores which are consistent with other fluorescent C-dots.[20,22] In summary, the pyrolysis of rice and doping of N and S heteroatoms into C-dots should have taken place at high temperature under microwave irradiation, resulting in the formation of *N,S*-C-dots covered with carboxylic acid, amido and alkyl sulfide moieties. These functional groups are potential linkers for attachment of therapeutic moieties for targeted drug delivery.
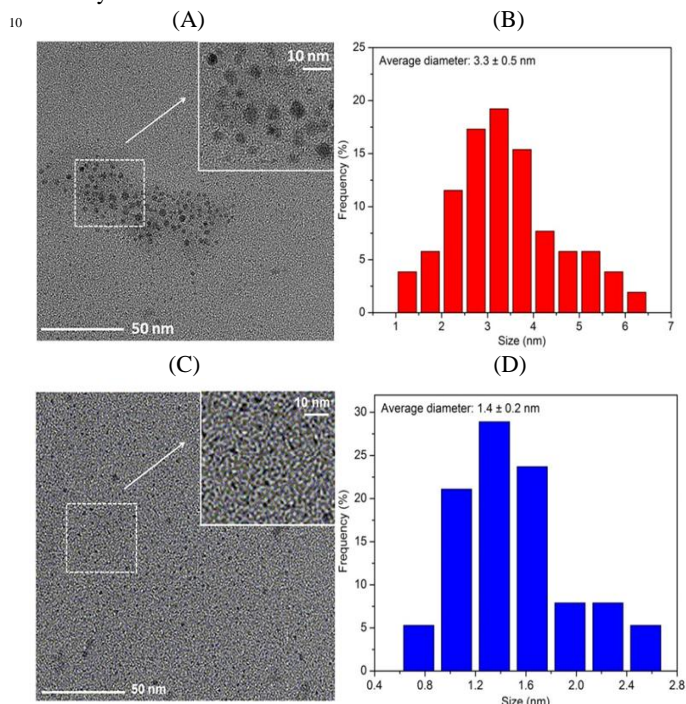

Fig. 3. (A) TEM image and (B) particle size distribution histogram of undoped C-dots. (C) TEM image and (D) particle size distribution histogram of *N,S*-C-dots

To gain further insight into the surface functional groups and element states of C-dots, XPS of C-dots were acquired. Fig. 1 and 2 depict the survey scan of the undoped C-dots and the *N,S*-C-dots, respectively. For the undoped C-dots, three peaks centred at 285.0, 400.5 and 532.3 eV associated with C1s, N1s and O1s are identified (Fig. 1A). For the *N,S*-C-dots, an additional peak at 165.0 eV attributing to S2p is observed (Fig. 2A), inferring the presence of S in the C-dots.[30] The peak associated with N1s of *N,S*-C-dots is much more intense than that of the undoped C-dots, indicating that a higher content of N in the C-dots. These results further confirm the incorporation of heteroatoms N and S from NAC into *N,S*-C-dots. Fig. 1B and 2B illustrate the C1s XPS spectra of the undoped C-dots and the *N,S*-C-dots, respectively. For the undoped C-dots, the C1s spectrum is deconvoluted into three peaks at 284.6, 286.2 and 287.9 eV corresponding to C=C, C–O and C=O, respectively.[31-34] For the *N,S*-C-dots, additional peaks at 283.9, 285.2 and 289.0 eV associated with C–S–C, C–N and O–C=O are observed.[31,35-37] Fig. 2C reveals the S2p XPS of *N,S*-C-dots. The S2p XPS could be fitted into two peaks at 163.4 and 164.8 eV corresponding to S2p$_{2/3}$ and S2p$_{1/3}$ C–S–C, respectively.[30,37] Again, these confirm the doping of N and S onto the surface of the as-synthesised *N,S*-C-dots. In summary, the XPS data show the presence of C=C, C–O and C=O surface-functionalities on the undoped C-dots whereas the C=C, C–O, C=O, C–S–C, C–N and O–C=O surface-functionalities are on the *N,S*-C-dots. Both XPS and IR confirm the surface of *N,S*-C-dots is co-doped with N and S atoms.
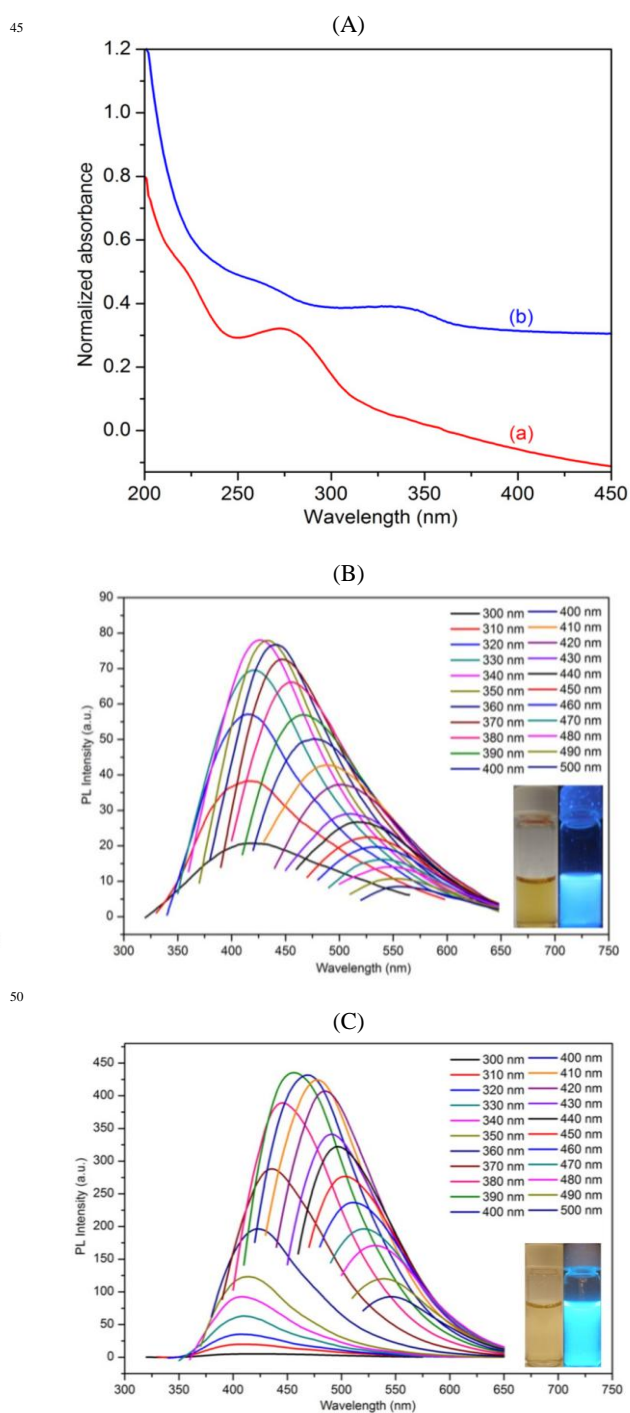

Fig. 4. (A) UV-vis absorption spectra of (a) undoped C-dots and (b) *N,S*-C-dots. Spectra are offset for ease of comparison. (B) and (C) are PL spectra at different λ$_{ex}$ 300–500 nm of undoped C-dots and *N,S*-C-dots, respectively. The insets display the images of undoped C-dots and *N,S*-C-dots under daylight and UV irradiation. The concentrations of C-dots are 0.50 mg/mL.

TEM has been used extensively as a powerful tool in the study of NPs from which the morphology and size can be identified. Fig. 3A and C shows the representative TEM images of the undoped C-dots and the *N,S*-C-dots, respectively. Both undoped C-dots and *N,S*-C-dots are mostly of spherical morphology and disperse rather evenly on the TEM grid surface. The corresponding histograms obtained by statistical analysis of

approximately 100 particles using the ImageJ software are displayed in Fig. 3B and D. The Gaussian fitting curves reveal that the corresponding particle size distributions of undoped C-dots and *N*,*S*-C-dots are 1.3–6.4 nm and 0.7–2.6 nm with average diameters of 3.3 ± 0.5 nm and 1.4 ± 0.2 nm, respectively. It is obvious that the *N*,*S*-C-dots are smaller than the undoped C-dots and the *N*,*S*-C-dots have narrower size range. In brief, doping N and S into C-dots could inhibit the growth of carbon core, allowing the formation of ultrasmall C-dots (< 2 nm).

In quest of exploring the optical properties of the as-prepared C-dots, the UV-vis absorption and PL spectra are acquired and depicted in Fig. 4. For the undoped C-dots, an absorption peak at 275 nm corresponding to the $n \rightarrow \pi^*$ transition of C=O bond and a shoulder peak at *ca.* 225 nm attributing to the $\pi \rightarrow \pi^*$ transition of the aromatic sp^2 domain (spectrum *a* in Fig. 4A) are observed.[38,39] For the *N*,*S*-C-dots (spectrum *b* in Fig. 4A), in addition to the $n \rightarrow \pi^*$ transition at 263 nm, a prominent absorption peak at 335 nm is found, probably attributing to the formation of excited defect surface states induced by the N and S heteroatoms.[40-42] Fig. 4B and C display the PL spectra of the undoped C-dots and the *N*,*S*-C-dots under various excitation wavelengths (λ_{ex}), respectively. The PL spectra are bathochromically shifted with the increase in the λ_{ex}, indicating that the PL band can be tuned by adjusting the λ_{ex}. The emission peaks (λ_{em}) are red-shifted from 412 to 558 nm for the undoped C-dots and from 415 to 545 nm for the *N*,*S*-C-dots when the λ_{ex} moves from 300 to 500 nm. The λ_{ex}-dependent PL behaviour is common with C-dots. This means that the λ_{em} can be tuned by just controlling the λ_{ex} without changing C-dots. The emission intensities of the *N*,*S*-C-dots are much stronger than that of the undoped C-dots. Obviously, doping N and S into the C-dots surface could introduce surface states with a concomitant effect of enhancing the fluorescence of C-dots.

The Φ_S of C-dots is determined†. The Φ_S excited at 340 nm is only 0.090% for the undoped C-dots (curve 1 in Fig. S3†). The Φ_S of the *N*,*S*-C-dots are 1.16 and 2.36% when excited at 340 and 390 nm (curves 2 and 3 in Fig. S3†), respectively using quinine sulfate as the reference. The Φ_S of *N*,*S*-C-dots is about 13–26 times of the undoped C-dots, indicating that doping N and S into C-dots could greatly improve its Φ_S. These results are consistent with a previous report that reduced C-dots have higher Φ_S than that of oxidised C-dots.[43] Our undoped C-dots contain higher oxygen content, *i.e.*, oxygenated functionalities (*vide supra*) and is therefore more oxidised than the *N*,*S*-C-dots.

HPLC separation of the as-synthesised *N*,*S*-C-dots

It has been reported that the surface-doped N and S atoms on C-dots are the main factors for enhancing the PL of C-dots.[30,44,45] As such, a series of C-dots were synthesised with different NAC/rice and then analysed by HPLC-FD. Fig. 5A depicts the chromatographic separation of the undoped C-dots and various as-synthesised *N*,*S*-C-dots products. On all chromatograms, numerous well separated peaks are observed, inferring that the as-synthesised C-dots are composed of different C-dots species. Our developed HPLC-FD can be successfully applied to separate complex C-dots samples. The solutes in the undoped C-dots exhibit very low detection signals (chromatogram *a*), indicating that without NAC the generated C-dots will have much weaker fluorescence emissions. Remarkably, with NAC (chromatograms *b–e*), peaks with much stronger detection signals are observed, inferring that C-dots doped with N and S possess stronger emissions. When the NAC/rice increases from 0.20 to 0.80, the signals of the later eluted peaks increase progressively, indicating that higher NAC/rice benefits the generation of C-dots with stronger fluorescence emissions. All these observations suggest

that the PL of C-dots is indeed governed by the NAC/rice in the synthesis. As too high NAC/rice (> 0.80) do not further improve the PL of the C-dots, only *N*,*S*-C-dots synthesised with 0.80 of NAC/rice (Fig. 5C) was used for comparison with the undoped C-dots (Fig. 5B). In order to achieve a better understanding of the passivation effect of NAC on C-dots, twelve of each separated fractions labelled in Fig. 5B and C of the undoped C-dots and the *N*,*S*-C-dots respectively were collected for further characterisation by MALDI-TOF MS, UV-vis absorption and PL spectroscopy.
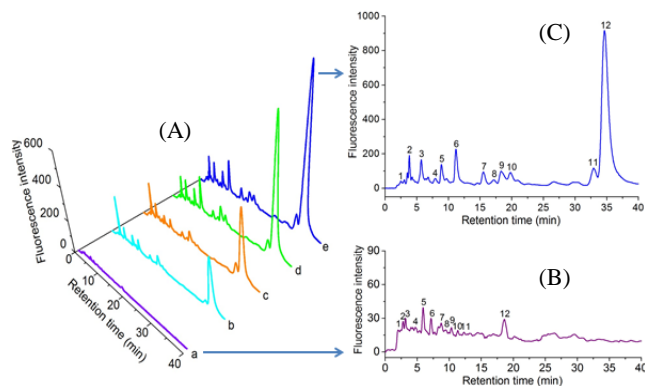

Fig. 5. Chromatograms of aqueous solutions of *N*,*S*-C-dots (1.0 mg/mL) synthesised with different mass ratios of NAC to rice: (a) 0.00, (b) 0.20, (c) 0.40, (d) 0.60, and (e) 0.80. (B) and (C) are the expanded chromatograms of undoped C-dots and *N*,*S*-C-dots synthesised with the mass ratio of NAC to rice at 0.00 and 0.80 respectively for clarity and ease of comparison. The chromatograms are acquired by monitoring the fluorescence detector at $\lambda_{ex}/\lambda_{em}$ of 340/400 nm.

Mass spectrometric analysis of HPLC fractions

Mass spectrometry was employed to gauge the structural information of the as-synthesised C-dots. Fig. S4† displays the MALDI-TOF MS of fractions 1–12 in the *N*,*S*-C-dots. The ion species of largest mass are labelled on all the MS with red asterisks. All the peak assignments are within the mass accuracy of the MALDI-TOF MS, *i.e.*, 1–2 mass units. The largest mass ions on the MS of the HPLC fractions are located within a narrow mass range 2189–2588 Da, indicating that the mass of the separated *N*,*S*-C-dots species do not show much variations. Their difference in retention on the C18 column is probably attributing to the variations of their surface-attached functionalities. The fragmentation patterns of their MS look very similar. Herein, fraction 12 was chosen as the representative *N*,*S*-C-dots species for clear assignment of their mass peaks as it displays the strongest fluorescence emission in Fig. 5C. Fig. 6A and B depicts the MALDI-TOF MS of fraction 12 and its expanded MS in the mass range 985–1385 Da, respectively. The highest mass ion is located at 2473 Da. A series of major mass spacing in the alternating mass units of 175 and 115 are identified on the expanded MS. We elucidate that the fragment (*m/z* 175) is due to the loss of a pyranose (glucose) unit. The fragment (*m/z* 115) is attributed to the loss of a $C_5H_7O_3$ molecule which is originally derived from a glucose unit ($C_6H_{10}O_5$, *m/z* 162) less a $-CH_2OH$ group (31) and an O atom (16). Since the carbon source of our C-dots is rice which comprises mainly amylopectin and amylose, it is possible that the *N*,*S*-C-dots contain some surface-attached residual glucose units and open ring pyranose structures (each less a $-CH_2OH$ group and an O atom) which are obviously derived from rice. In addition, a series of minor mass spacing in the mass units of 58, 45, 43, 33, 18, and 15 corresponding to the loss of a $-CH_3CONH$, $-COOH$, $-CH_3CO$, $-SH$, H_2O, and $-NH$

or –CH$_3$ moieties are identified. These observations further confirm the incorporation of heteroatoms N and S into the *N*,*S*-C-dots and their surfaces are composed of carboxylic acid, amide and alkyl sulfide functionalities.


(A)

(B)
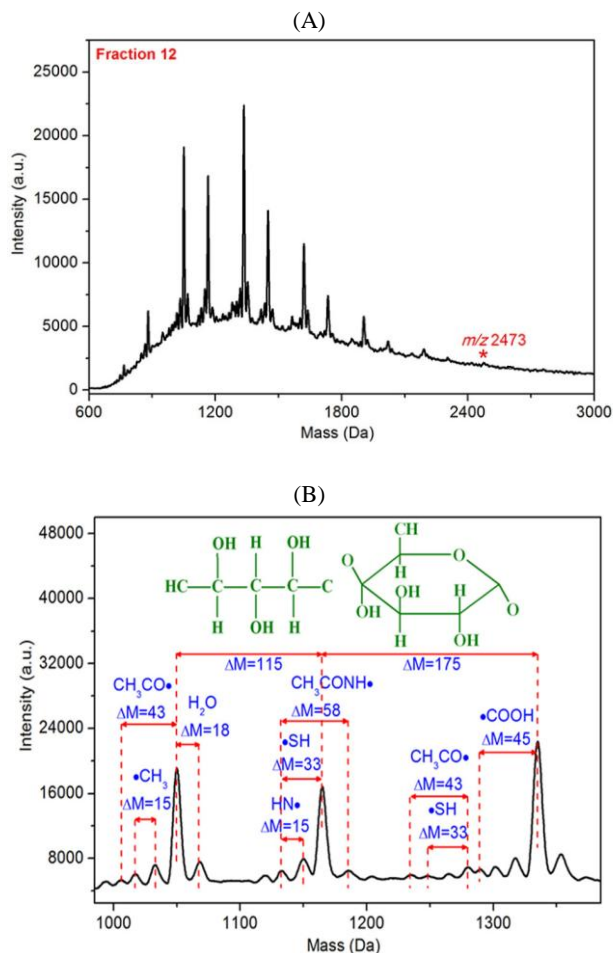
Fig. 6. (A) MALDI-TOF MS and (B) expanded MS in the mass range 985–1385 Da of fraction 12 in *N*,*S*-C-dots.

For comparison, the MS of fraction 12 in the undoped C-dots possessing the strongest fluorescence emission was acquired and displayed in Fig. 7. The MS feature is different from that of the *N*,*S*-C-dots. A large number of higher mass fragments are observed for the undoped C-dots. The highest mass ion is located at 7705 Da (Fig. 7A) which is about 3 times that of the *N*,*S*-C-dots (Fig. 6A), indicating that the *N*,*S*-C-dots is smaller (lighter) than the undoped C-dots which is consistent with their sizes. The average size of the undoped C-dots is about 2.4 times that of the *N*,*S*-C-dots (Fig. 3). However, the mass spectral feature in the mass range 1000–3000 Da shows some similarity to that of the *N*,*S*-C-dots. Fig. 7B depicts the expanded MS of fraction 12 in the mass range 1000–1400 Da. Fragments of *m/z* 115 and 175 are common, indicating that the chemical composition of the undoped C-dots is similar to that of the *N*,*S*-C-dots since both are derived from the same carbon source, *i.e.*, rice. Again, the fragment (*m/z* 115) is from the loss of a C$_5$H$_7$O$_3$ molecule and the fragment (*m/z* 115) is from a glucose unit (C$_6$H$_{10}$O$_5$, *m/z* 162) minus a –CH$_2$OH group (31) and an O atom (16). Also a series of minor mass spacing in the mass units of 18, 17, and 15 corresponding to the loss of H$_2$O, –OH, and –CH$_3$ moieties are also found. Interestingly, at the higher mass range 3500–7000 Da, regular mass spacings of 131 corresponding to a C$_5$H$_7$O$_4$ unit are

found for the undoped C-dots (Fig. 7A) which is not observed in the MS of the *N*,*S*-C-dots.

(A)

(B)

(C)
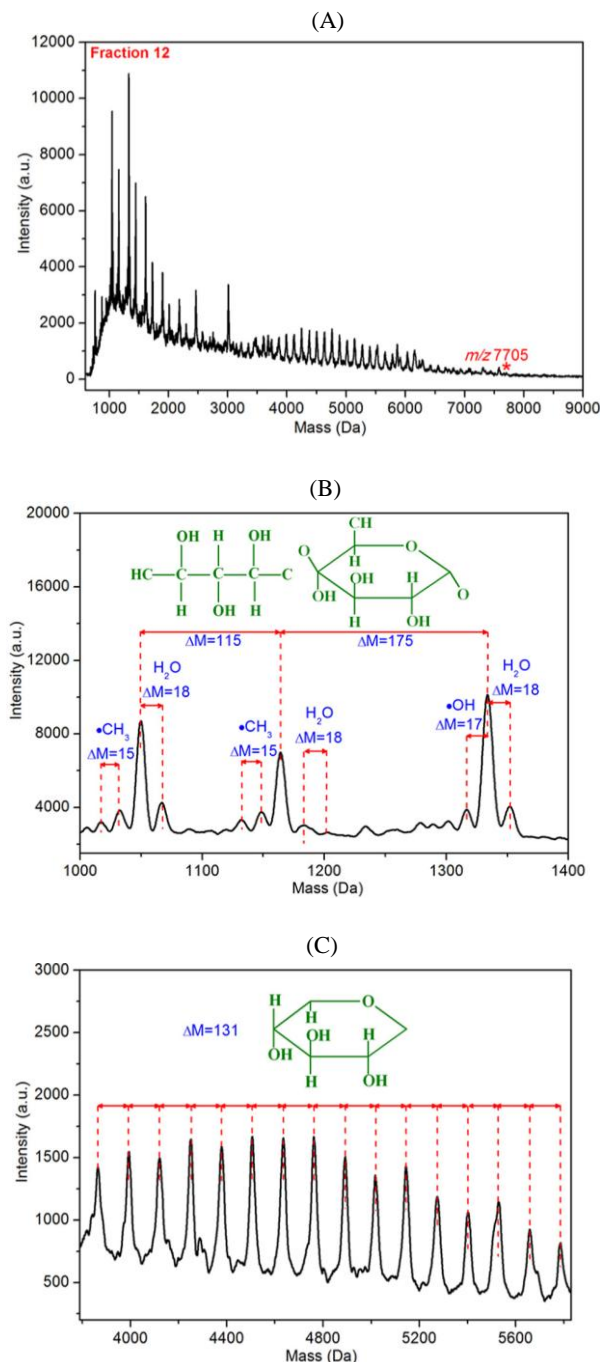
Fig. 7. (A) MALDI-TOF MS of fraction 12 in the undoped C-dots. (B) and (C) are expanded MS in the mass ranges 1000–1400 and 3790–5830 Da, respectively.

Fig. 7C displays the expanded MS of fraction 12 in the undoped C-dots in the mass range 3790–5830 Da. We speculate that the fragment (*m/z* 131) is derived from the residual amylopectin on the undoped C-dots surface. To further confirm this, the dissolved amylopectin obtained by sonication of rice powder in DDI water was subjected to MS analysis and the results are depicted in Fig. S5A†. The highest mass ion of rice is located at 9428 Da. The MS displays very regular mass spacings of fragments (*m/z* 162). Fig. S5B and C† show the expanded MS

in the mass range 1190–3230 and 3210–5250 Da, respectively. Numerous evenly distributed mass spacing in mass units of 162 corresponding to a glucose unit ($C_6H_{10}O_5$) are identified on both expanded MS, indicating that the rice sample is mainly composed of amylopectin and amylose. As such, we can deduce that the 131 mass unit in the MS of the undoped C-dots is also a fragment of amylopectin corresponding to the loss of a $-CH_2OH$ group (31) from a glucose unit (162). These results suggest that synthesis without NAC fails to completely carbonise amylopectin/amylose but NAC can greatly improve the carbonisation of rice under our experimental conditions. Other attributes of the N,S-C-dots are that they possess stronger fluorescence and are smaller in size as compared to the undoped C-dots.

Absorption and photoluminescence of HPLC fractions of N,S-C-dots

To further understand the optical properties of the C-dots species in the as-synthesised C-dots products, the absorption and PL spectra of the HPLC fractions of the undoped C-dots and the N,S-C-dots are displayed in Fig. S6† and Fig. 8, respectively. For the undoped C-dots, all fractions exhibit typical absorption spectral characteristics of the unseparated undoped C-dots mixture with an absorption peak between 250 and 285 nm corresponding to the $n \rightarrow \pi^*$ transition of C=O bond (Fig. S6A†).[38,39] However, their spectral features are different, inferring that they represent different C-dots species in the undoped C-dots product. As expected for reversed-phase HPLC separation, the earlier eluted solutes should have higher polarity than that of the later eluted ones. The earlier eluted fractions 1–10 display more prominent absorption bands at 250–285 nm corresponding to the $n \rightarrow \pi^*$ transition of C=O bond, inferring that they contain more surface-attached oxygenated functionalities (*e.g.*, carboxylic and carbonyl groups) whereas the later fractions 11 and 12 probably contain less oxygenated groups or more sp^2 domains in the C-dots. Upon excitation at 340 nm, fractions 1–12 show emission bands in the range 410–424 nm (Fig. S6B†) which is consistent with that of the unseparated ones. For the N,S-C-dots, although all fractions exhibit typical absorption spectral characteristics of the unseparated N,S-C-dots mixture, their spectra are more distinctive. They show shoulder or absorption bands between 240–268 nm assigned to the $n \rightarrow \pi^*$ transition of C=O bond[38,39] and another absorption bands *ca.* 300–360 nm ascribed to the excited defect surface states induced by the heteroatoms N and S (Fig. 8A).[40-42] These absorption bands are prominent and hypsochromically shifted from 347 to 323 nm for fraction 2 to 11. Fractions 2, 3, 5–7, and 9–12 exhibit more distinctive double absorption bands, not observed before, corresponding to the $n \rightarrow \pi^*$ transition of C=O bond and the defect surface state induced by N and S atoms. For the later eluted fractions 7–12, the $n \rightarrow \pi^*$ band is less prominent, indicating that they possess less C=O and COOH groups; thus, they are less polar and retain better on the C18 column. When fractions 1–12 are excited at 340 nm, the emission spectrum is bathochromically shifted from 382 to 423 nm (Fig. 8B). These observations indicate that each C-dots species displays its unique spectral properties and their co-existence in a C-dots product would also contribute to the λ_{ex}-dependent PL behaviour of the as-synthesised C-dots.

Table 1. Quantum yield (Φ_S) of HPLC fractions 1–12 in N,S-C-dots

Fraction	1	2	3	4	5	6	7	8	9	10	11	12
Φ_S(%)	0.81	0.91	0.82	1.85	2.05	1.37	2.03	1.43	1.97	1.46	2.36	7.37

Table 1 summarises the Φ_S of fractions 1–12 in the N,S-C-dots upon excitation at 390 nm and using quinine sulfate as the reference. Apparently, fraction 12 displays the highest Φ_S (7.37%)

which is about 3 times that of the unseparated N,S-C-dots mixture (2.36%). Our results demonstrate that some absorbing species displaying no or low PL are also present in the N,S-C-dots mixture.[46] By HPLC fractionation, C-dots species exhibiting appreciable PL performance could be isolated and possibly be a promising cellular imaging probe.
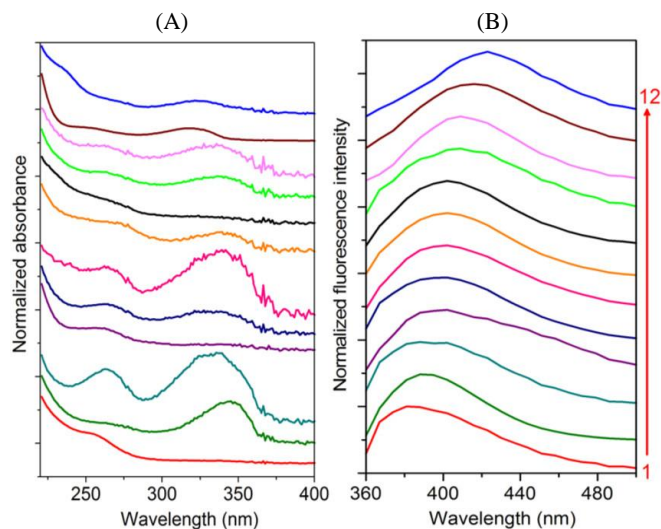

Fig. 8. (A) and (B) are the absorption and fluorescence emission spectra of peak 1–12 (from bottom to top) of N,S-C-dots in Fig. 5C, respectively.

Conclusions

For the first time, N,S-doped C-dots have been synthesised from a fast, simple and "green" route with rice and NAC as the precursors. The effect of NAC on the synthesis of C-dots was studied by FTIR, XPS, TEM, UV absorption and PL spectroscopy coupled with modern analytical HPLC methodology. It is found that higher NAC/rice favours the production of C-dots with stronger emissions. By collecting the HPLC fractions of undoped C-dots and N,S-C-dots, the spectral properties and surface-attached functionalities of the individual C-dots species could be more precisely studied by MS, UV absorption and PL spectroscopy. It is found that the PL properties of C-dots are not only determined by particle size but also the structural changes induced by doping with heteroatoms into C-dots. The absorption band at 275 nm corresponding to the $n \rightarrow \pi^*$ transition of C=O bond of the undoped C-dots produces rather weak fluorescence emission. By contrast, when C-dots is doped with heteroatoms N and S, its absorption band could bathochromatically shift to 335 nm attributing to the formation of excited defect surface state which can enhance fluorescence emission. Moreover, our HPLC analysis has demonstrated that an as-synthesised N,S-C-dots product comprises numerous C-dots species. They are similar in particle size and mass but exhibit unique PL properties and Φ_S, inferring that particle size is not the key parameter that determines the PL properties of the N,S-C-dots species. It is anticipated that our developed method will open new avenues in synthesising strongly emitted C-dots from biomaterials. It also exhibits a potential of fast, easy and inexpensive large-scale production of C-dots from natural material.

Acknowledgments

Notes and references

[a]Partner State Key Laboratory of Environmental and Biological Analysis, and Department of Chemistry, Hong Kong Baptist University, 224 Waterloo Road, Kowloon Tong, Hong Kong SAR, China. E-mail: mfchoi@hkbu.edu.hk
[b]Institute of Environmental Science, and School of Chemistry and Chemical Engineering, Shanxi University, Taiyuan 030006, China.
[c]School of Civil & Environmental Engineering, and National International Cooperation Base on Environment and Energy, University of Science and Technology Beijing, 30 Xueyuan Road, 100083 Beijing, China. E-mail: yaojun@ustb.edu.cn
[‡]Exchange student on visit to Hong Kong Baptist University.

†Electronic supplementary information (ESI) available: elemental analysis data, IR spectra of C-dots, rice and NAC, determination of quantum yield, plots of integrated PL intensity against absorbance of undoped C-dots and *N,S*-C-dots, MALDI-TOF MS of HPLC fractions of *N,S*-C-dots, MS and expanded MS of rice, and absorption and PL spectra of HPLC fractions of undoped C-dots. See DOI: 10.1039/

1   S. N. Baker and G. A. Baker, *Angew. Chem. Int. Ed*., 2010, **49**, 6726-6744.
2   A. B. Bourlinos, A. Stassinopoulos, D. Anglos, R. Zboril, M. Karakassides and E. P. Giannelis, *Small*, 2008, **4**, 455-458.
3   A. B. Bourlinos, A. Stassinopoulos, D. Anglos, R. Zboril, V. Georgakilas and E. P. Giannelis, *Chem. Mater*., 2008, **20**, 4539-4541.
4   L. Cao, X. Wang, M. J. Meziani, F. Lu, H. Wang, P. G. Luo, Y. Lin, B. A. Harruff, L. M. Veca, D. Murray, S.-Y. Xie and Y.-P. Sun, *J. Am. Chem. Soc*., 2007, **129**, 11318-11319.
5   Y.-P. Sun, B. Zhou, Y. Lin, W. Wang, K. A. S. Fernando, P. Pathak, M. J. Meziani, B. A. Harruff, X. Wang, H. Wang, P. G. Luo, H. Yang, M. E. Kose, B. Chen, L. M. Veca and S.-Y. Xie, *J. Am. Chem. Soc*. 2006, **128**, 7756-7757.
6   S.-T. Yang, L. Cao, P. G. Luo, F. Lu, X. Wang, H. Wang, M. J. Meziani, Y. Liu, G. Qi and Y.-P. Sun, *J. Am. Chem. Soc*., 2009, **131**, 11308-11309.
7   L. Cao, X. Wang, M. J. Meziani, F. Lu, H. Wang, P. G. Luo, Y. Lin, B. A. Harruff, L. M. Veca, D. Murray, S.-Y. Xie and Y.-P. Sun, *J. Am. Chem. Soc.*, 2007, **129**, 11318-11319.
8   S. C. Ray, A. Saha, N. R. Jana and R. Sarkar, *J. Phys. Chem. C*, 2009, **113**, 18546-18551.
9   B. Zhu, S. Sun, Y. Wang, S. Deng, G. Qian, M. Wang and A. Hu, *J. Mater. Chem. C*, 2013, **1**, 580-586.
10   J. Lu, J.-X. Yang, J. Wang, A. Lim, S. Wang and K. P. Loh, *ACS Nano*, 2009, **3**, 2367-2375.
11   X. Wang, L. Cao, F. Lu, M. J. Meziani, H. Li, G. Qi, B. Zhou, B. A. Harruff, F. Kermarrec and Y.-P. Sun, *Chem. Commun*., 2009, 3774-3776.
12   S.-T. Yang, X. Wang, H. Wang, F. Lu, P. G. Luo, L. Cao, M. J. Meziani, J.-H. Liu, Y. F. Liu, M. Chen, Y. Huang and Y.-P. Sun, *J. Phys. Chem. C*, 2009, **113**, 18110-18114.
13   S. Sahu, B. Behera, T. K. Maiti and S. Mohapatra, *Chem. Commun*., 2012, **48**, 8835-8837.
14   D. Pan, J. Zhang, Z. Li and M. Wu, *Adv. Mater*., 2010, **22**, 734-738.
15   P.-C. Hsu and H.-T. Chang, *Chem. Commun*., 2012, **48**, 3984-3986.
16   D. Pan, J. Zhang, Z. Li, C. Wu, X. Yan and M. Wu, *Chem. Commun*., 2010, **46**, 3681-3683.
17   S. Zhu, Q. Meng, L. Wang, J. Zhang, Y. Song, H. Jin, K. Zhang, H. Sun, H. Wang and B. Yang, *Angew. Chem. Int. Ed*., 2013, **52**, 3953-3957.
18   A. Jaiswal, S. S. Ghosh and A. Chattopadhyay, *Chem. Commun*., 2012, **48**, 407-409.
19   H. Zhu, X. Wang, Y. Li, Z. Wang, F. Yang and X. Yang, *Chem. Commun*., 2009, 5118-5120.
20   X. Wang, K. Qu, B. Xu, J. Ren and X. Qu, *J. Mater. Chem*., 2011, **21**, 2445-2450.
21   Y. Li, X. Zhong, A. E. Rider, S. A. Furman and K. Ostrikov, *Green Chem*., 2014, DOI: 10.1039/C3GC42562B.
22   J. Xu, Y. Zhou, S. Liu, M. Dong and C. Huang, *Anal. Methods*, 2014, DOI: 10.1039/C3AY41715H.
23   Z. Zhang, J. Hao, J. Zhang, B. Zhang and J. Tang, *RSC Adv*., 2012, **2**, 8599-8601.
24   X. Qin, W. Lu, A. M. Asiri, A. O. Al-Youbi and X. Sun, *Catal. Sci. Technol*., 2013, **3**, 1027-1035.
25   A. Mewada, S. Pandey, S. Shinde, N. Mishra, G. Oza, M. Thakur, M. Sharon and M. Sharon, *Mater. Sci. Eng. C*, 2013, **33**, 2914-2917.
26   D. Sun, R. Ban, P.-H. Zhang, G.-H. Wu, J.-R. Zhang and J.-J. Zhu, *Carbon*, 2013, **64**, 424-434.
27   Z. L. Wu, P. Zhang, M. X. Gao, C. F. Liu, W. Wang, F. Leng and C. Z. Huang, *J. Mater. Chem. B*, 2013, **1**, 2868-2873.
28   Z.-Q. Xu, L.-Y. Yang, X.-Y. Fan, J.-C. Jin, J. Mei, W. Peng, F.-L. Jiang, Q. Xiao and Y. Liu, *Carbon*, 2014, **66**, 351-360.
29   W. Wang, Y. Li, L. Cheng, Z. Cao and W. Liu, *J. Mater. Chem. B*, 2014, **2**, 46-48.
30   Y. Dong, H. Pang, H. B. Yang, C. Guo, J. Shao, Y. Chi, C. M. Li and T. Yu, *Angew. Chem. Int. Ed*., 2013, **52**, 7800-7804.
31   Z. Yang, M. Xu, Y. Liu, F. He, F. Gao, Y. Su, H. Wei and Y. Zhang, *Nanoscale*, 2014, **6**, 1890-1895.
32   S.-A. Wohlgemuth, R. J. White, M.-G. Willinger, M.-M. Titirici and M. Antonietti, *Green Chem*., 2012, **14**, 1515-1523.
33   C. Bureau, F. Valin, G. Lecayon, J. Charlier and V. Detalle. *J. Vac. Sci. Technol. A*, 1997, **15**, 353-364.
34   F. Beguin, I. Rashkov, N. Manolova, R. Benoit, R. Erre and S. Delpeux, *Eur. Polym. J*., 1998, **34**, 905-915.
35   S. Wan, L. Wang and Q. Xue, *Electrochem. Commun*., 2010, **12**, 61-65.
36   S. Liu, J. Tian, L. Wang, Y. Zhang, X. Qin, Y. Luo, A. M. Asiri, A. O. Al-Youbi and X. Sun. *Adv. Mater*., 2012, **24**, 2037-2041.
37   J. Liang, Y. Jiao, M. Jaroniec and S. Z. Qiao, *Angew. Chem*. 2012, **124**, 11664-11668.
38   G. Eda, Y.-Y. Lin, C. Mattevi, H. Yamaguchi, H.-A. Chen, I.-S. Chen, C.-W. Chen and M. Chhowalla, *Adv. Mater*., 2010, **22**, 505-509.
39   J. I. Paredes, S. Villar-Rodil, A. Martínez-Alonso and J. M. D. Tascón, *Langmuir*, 2008, **24**, 10560-10564.
40   Wang, L. Cao, S.-T. Yang, F. Lu, M. J. Meziani, L. Tian, K. W. Sun, M. A. Bloodgood and Y.-P. Sun, *Angew. Chem. Int. Ed*., 2010, **49**, 5310-5314.
41   P. Anilkumar, X. Wang, L. Cao, S. Sahu, J.-H. Liu, P. Wang, K. Korch, K. N. Tackett II, A. Parenzan and Y.-P. Sun, *Nanoscale*, 2011, **3**, 2023-2027.
42   Y.-P. Sun, X. Wang, F. Lu, L. Cao, M. J. Meziani, P. G. Luo, L. Gu and L. M. Veca, *J. Phys. Chem. C*, 2008, **112**, 18295-18298.
43   S. K. Das, Y. Liu, S. Yeom, D. Y. Kim and C. I. Richards, *Nano Lett.*, 2014, **14**, 620-625.
44   Q. Liang, W. Ma, Y. Shi, Z. Li and X. Yang, *Carbon*, 2013, **60**, 421-428.
45   Y. Xu, M. Wu, Y. Liu, X.-Z. Feng, X.-B. Yin, X.-W. He and Y.-K. Zhang, *Chem. Eur. J*., 2013, **19**, 2276-2283.
46   J. C. Vinci, I. M. Ferrer, S. J. Seedhouse, A. K. Bourdon, J. M. Reynard, B. A. Foster, F. V. Bright and L. A. Colón, *J. Phys. Chem. Lett*., 2013, **4**, 239-243.